Analytic temperature evaluation and process forces estimation for the RARR process of flat rings

Publisher:
AIP Publishing

Published version:
DOI: 10.1063/1.4963527

Analytic temperature evaluation and process forces estimation for the RARR process of flat rings

L. Quagliato and G. A. Berti

Citation: AIP Conference Proceedings **1769**, 130008 (2016); doi: 10.1063/1.4963527
View online: http://dx.doi.org/10.1063/1.4963527
View Table of Contents: http://scitation.aip.org/content/aip/proceeding/aipcp/1769?ver=pdfcov
Published by the AIP Publishing

Analytic temperature evaluation and process forces estimation for the RARR process of flat rings

L. Quagliato[1, a)] and G.A. Berti[1, b)]

[1]*University of Padua – Department of Management and Engineering*
Stradella San Nicola 3 – 36100 Vicenza (Italy)

[a)] Corresponding author: luca.quagliato@studenti.unipd.it
[b)] guido.berti@unipd.it

Abstract. Two different analytical models are derived for the estimation of the temperature drop in the two deformation stages of radial-axial ring rolling process of flat rings. The temperature estimation, along with previous results regarding geometry, strain and strain rate, is used to calculate the variation of the flow stress of the material during the process and accordingly to derive the process forces, utilizing different forces estimation models already available in the literature.

INTRODUCTION

The RARR (radial-axial ring rolling) process, schematized in Fig. 1a, is a coupled thermo-mechanical forming process [1] where the contact of the tools with the ring, as well as the heat exchange with the environment, cause a temperature drop resulting in an increase of both material flow stress and forces required to deform the ring. Thus, the estimation of the process forces has a wide relevance to process engineers since it can determine the feasibility of process itself and also influence the choice of the ring rolling mill. Although so far much effort has been spent by different authors to analyze the process forces using different methods, such as: FE methodology by Zhou et al. [1], Slab method by Parvizi et al. [2], Upper bound analysis by Parvizi et al. [3] and also Slip line method by Hawkyard et al. [4], an analytical way to estimate the temperature evolution along the process, aimed to calculate the flow stress of the material and accordingly derive the radial forming force, seems to be missing in the literature.

The purpose of this paper is to derive an analytical model able to foresee the temperature drop caused by conductive, convective and radiant heat exchange and, together with prediction of geometry and strains proposed by the authors [5, 6], to estimate the flow stress of the material and accordingly to derive the process forces, utilizing different force models available in the literature [4, 7, 8, 9]. The verification of the proposed model is based on authors' FE simulation, which have been compared with the results of the above-mentioned literature forces models, where authors' flow stress estimation has been used.

MATHEMATICAL MODEL DEFINITION

During the process, the whole surface of ring is interested by radiant and convective heat exchange without any inversion of the heat flow, thus the adoption of lumped models to calculate the temperature drop caused by these two phenomena is reasonable and the reliability of this assumption will be demonstrated in the result paragraph.

As concerns the conductive heat exchange, the contact is limited to a small portion of the surface: this area is continuously varying and, after a short contact time, the cooled portion of the ring is heated up by the not-cooled inner core, where the temperature variation is very small. Moreover, the contact in the mandrel-main roll gap creates a heat flow prevalent in the radial direction. As concerns the heat exchange in axial rolls gap, the contact area, as well as the contact time, are different and the heat flow is prevalent in the axial direction.

ESAFORM 2016
AIP Conf. Proc. 1769, 130008-1–130008-6; doi: 10.1063/1.4963527
Published by AIP Publishing. 978-0-7354-1427-3/$30.00

A detailed modellization of these phenomena is out of the scope of this preliminary paper, where a lumped model has been extended also to the conductive heat exchange, separating the averaged contribution of mandrel-main roll gap and of axial rolls gap in a complete round of the ring rotation.

The proposed model decouples the four heat exchange phenomena applying them in a sort of sequence of heat transfer steps (Fig. 1b) where the temperature entering in step j is the one exiting from step j-1. At each round of the ring, the heat transfer is modeled as: i) contact heat transfer in the mandrel gap; ii) convective and radiant heat transfer during the rotation from the mandrel gap to the axial rolls gap; iii) contact heat transfer in the axial rolls gap; vi) convective and radiant heat transfer during the rotation from the axial rolls gap to the mandrel gap.

The following models are related to the conductive heat exchange whereas convective and radiant are based on lumped models proposed by Newton and Stefan-Boltzmann since their influence on temperature drop is limited.

Conductive heat exchange model for the mandrel-main roll gap

The lumped model for the estimation of the heat exchange in the mandrel-main roll gap has to be applied only on the area and volume really interested by the contact heat transfer, which are continuously varying during the process.

Due to the configuration of the contact zone, Fig. 2a, and to the assumption of a lumped model, the general differential equation of heat transfer is simplified as in (1), thanks to independency of the temperature form the position and to dependency of the heat exchange only on the contact with the tools.

In (1) the tools temperature T_T is considered as constant and the differential equation can easily be solved separating the variables under the hypothesis that A (heat exchange area), C (specific heat capacity), ρ (density), V and HTC (heat transfer coefficient) are constant during the integration interval.

$$\frac{dT}{dt} = \frac{A \cdot HTC}{C\rho V}\left(T - T_T\right) \tag{1}$$

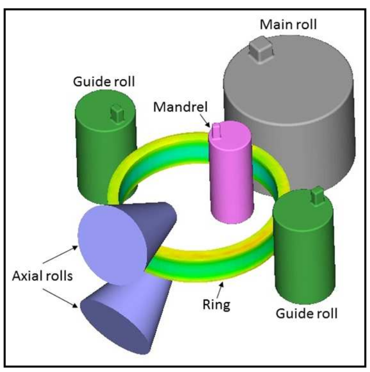

(a)

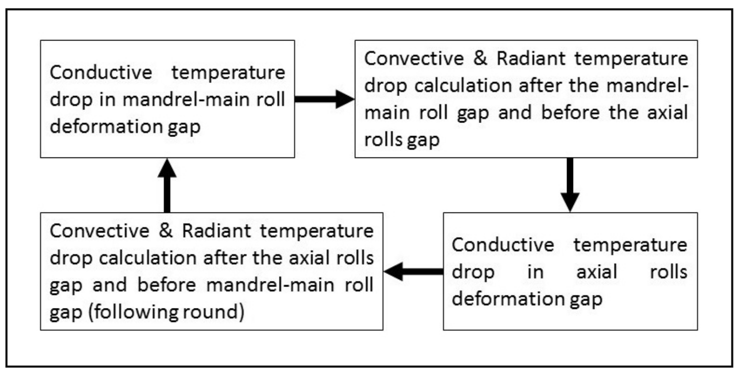

(b)

FIGURE 1. (a) radial-axial ring rolling (RARR) process scheme; (b) Iterative scheme for the calculation of the temperature.

Since the contact arc is small compared with the diameters of the ring, the projection of the contact arc is considered to have a common value for both mandrel side and main roll side. The projection of the contact arc between ring and tools, L_c (Fig. 2.a), can be estimated based on previous literature studies [2] and the center angle relevant to the inner ring circumference can be determined by Eq. (2), where r represents the inner radius of the ring.

The average contact time, (3), can be approximated as the time to complete half round multiplied by center angle (2) divided by π, where t_i is the time required to complete the considered i-round.

$$\alpha_{\mathrm{M}} = \arcsin\left(\frac{L_c}{r}\right) \tag{2}$$

$$t_M = \frac{t_i}{2}\frac{\alpha_{\mathrm{M}}}{\pi} \tag{3}$$

The heat exchange area at the mandrel side is estimated as a cylindrical surface corresponding to an arc having α_{mand} as vertex angle, (4), where α_{mand} is the arcsine function of the ratio between L_c and the mandrel radius R_M. Besides h_{avg} is the average height of the slice between the beginning and the end of the deformation gap.

$$A_M = \alpha_{mand} \cdot R_M \cdot h_{avg} \tag{4}$$

Along the ring rolling process the area interested by the heat exchange, as well as the volume affected by the conduction, continuously change hence, to overcome the difficulties of the calculation of these areas and volumes, authors have chosen to refer the heat transfer during half round of the ring as the conduction heat transfer acting on a volume equal to the volume of half ring adopting an heat exchange area equal to the undeformed inner surface of half ring for a duration of contact equal to the contact time defined in (3). Since the contact time defined in (3) is based on the deformed geometry of the ring whereas the contact heat transfer is based on the undeformed geometry, a correction factor must be introduced to take into account the difference between the undeformed and deformed geometry of the ring. This correction factor can be written as the ratio between the mandrel heat exchange area A_M and the corresponding undeformed contact area at the inner surface of the ring, $A_{indef,M}$, as shown in (5).

$$\eta_M = \frac{A_M}{A_{indef,M}} = \frac{\alpha_M \cdot R_M \cdot h_{avg}}{(\alpha_{\text{int,M}} \cdot r \cdot h_{avg})} \tag{5}$$

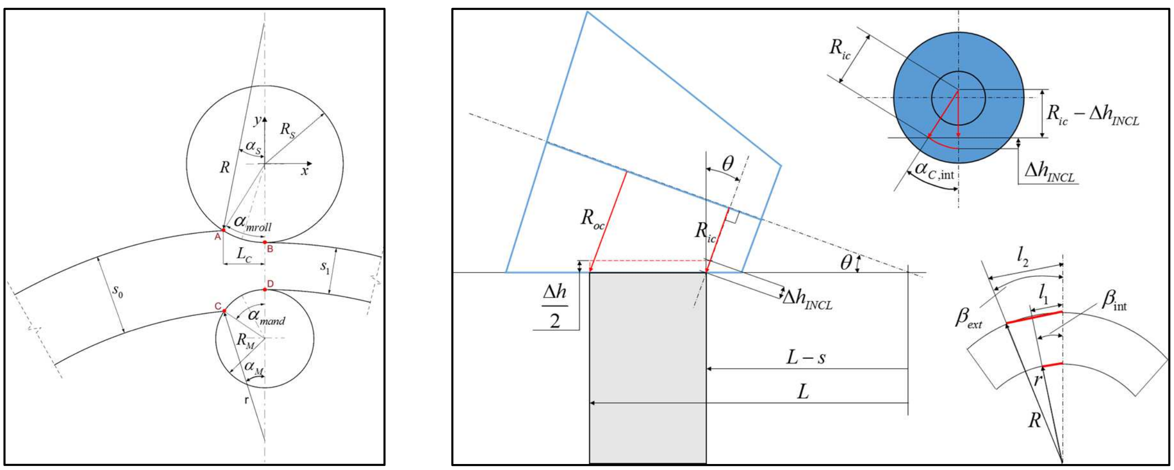

(a) (b)

FIGURE 2. (a) Mandrel-main roll contact scheme. (b) Axial rolls contact scheme.

The relevant parameters for the main-roll side have the following notations: R, α_S, α_{mroll}, t_S, A_S, $A_{indef,S}$, η_S and can be derived following the same equations and considerations previously presented. Having calculated the exchange areas for both inner and outer radius, their weighted sum based on their relevant contact time is derived as in (6).

$$A_{equiv,MS} \cdot t_{MS} = \frac{A_{\text{int}}}{2} \cdot t_M \cdot \eta_M + \frac{A_{ext}}{2} \cdot t_S \cdot \eta_S \tag{6}$$

Where A_{int} and A_{ext} are the undeformed inner and outer area of the ring respectively. The temperature drop caused by the passage in the mandrel-main roll deformation gap is estimated as in Eq. (7) where HTC represents the conductive global heat transfer coefficient between tools and ring and T_T is the temperature of the tools.

$$T_{MS} = (T - T_T) \cdot \exp\left(\frac{2 \cdot A_{equiv,MS} \cdot t_{MS} \cdot HTC}{C \rho V} \right) \tag{7}$$

Conductive heat exchange model for the axial rolls gap

For the axial rolls gap a new formulation for the contact arc must be developed and the first consideration which must be done is that the vertical reduction represented by the $\Delta h = h_1 - h_0$ must be projected onto a line orthogonal to axial rolls rotational axis, as shown in Eq. (8) and Fig. 2b, where θ represents half of the vertex angle of the cone.

$$\Delta h_{INCL} = \frac{\Delta h}{2}\cos\theta \tag{8}$$

Considering the inner and outer surface of the ring, they will contact the axial rolls at two different curves, which can be approximated by two arcs of circumferences whose centers are along the axis of the cone and the relevant radii are R_{ic} and R_{ec} (9), as shown in Fig. 2b.

$$R_{ic} = \left(L_0 - s\right)\sin\theta \ , \ R_{oc} = L_0 \sin\theta \tag{9}$$

The center angles, $\alpha_{C,int}$ and $\alpha_{C,ext}$, related to the radii defined by (9), can be estimated using Eq. (10) where R_{ic} must be used in case of inner contact whereas R_{oc} shall be used in case of outer contact.

$$\alpha_{\text{int,C}} = \arccos\left(\frac{R_{ic} - \Delta h_{INCL}}{R_{ic}}\right) \tag{10}$$

The length of the relevant arcs is the product between the center angle ($\alpha_{C,int}$ or $\alpha_{C,ext}$) and the radius (R_{ic} or R_{oc}) and it can be distributed on the inner circumference of the ring, or on the outer circumference, resulting in two arcs of circumference with ring inner and outer radius, r or R respectively, as also shown in Fig. 2b.

The center angles related to these arcs, relevant for inner and outer radius of the ring, can be estimated as in (11).

$$\beta_{\text{int}} = \frac{\alpha_{\text{C,int}} \cdot R_{ic}}{r} \ , \ \beta_{ext} = \frac{\alpha_{C,ext} \cdot R_{ec}}{R} \tag{11}$$

Having calculated all the relevant parameters for both inner and outer contact between cones and ring, the contact area of one cone with the ring can be approximated to the area of a curvilinear trapezoid as in (12).

$$A_{cont,cone} = \left(\beta_{\text{int}} \cdot r + \beta_{ext} \cdot R\right) \cdot \frac{s_{avg}}{2} \tag{12}$$

The contact time for the axial roll deformation gap, t_C, is estimated using the same formulation of Eq. (3) multiplied by a factor which is the ratio between the cone contact area $A_{cont,cone}$ and the upper area of the ring, A_{sup}, evaluated using the average values of inner and outer radius of the ring between the onset and the end of the contact zone. For the calculation of the equivalent contact area between rings and cones, authors suggest to use a parabolic interpolation function between the onset and end of the contact zone to estimate the variation of the contact inner and outer radius of the ring, resulting in $R_{med,par}$, and $r_{med,par}$, for the inner and outer radius respectively.

Afterwards, the temperature drop caused by the contact between tools and ring in the axial rolls deformation gap is estimated as in Eq. (14).

$$A_{equiv,C} = \pi \cdot \left(R_{med,par}{}^{2} - r_{med,par}{}^{2}\right) \tag{13}$$

$$T_{AR} = \left(T - T_T\right) \cdot \exp\left(\frac{2 \cdot A_{equiv,C} \cdot t_C \cdot HTC}{C\rho V}\right) \tag{14}$$

THE RESULTS OF THE EXPERIMENTAL CAMPAIGN

The experimental campaign has been performed on five rings with different ratio (from 2.67 to 0.42) between final height and final thickness to test the reliability of the model for a wide range of different rings configurations.

The summary of the simulation cases is given in Table 1, where blank and final ring dimensions are reported.

TABLE 1. Ring cases dimensions.

	Ring 1	Ring 2	Ring 3	Ring 4	Ring 5
d_0 [mm]	325.0	550.0	325.0	325.0	325.0
D_0 [mm]	607.8	1086.0	728.0	814.7	1242.9
s_0 [mm]	141.4	268.0	201.5	244.8	459.0
h_0 [mm]	233.2	438.0	201.5	184.5	249.8
d_F [mm]	950.0	1000.0	800.0	560.0	750.0
D_F [mm]	1100.0	1400.0	1100.0	1000.0	1600.0
s_F [mm]	75.0	200.0	150.0	220.0	425.0
h_F [mm]	200.0	400.0	150.0	150.0	180.0
h_F / s_F [-]	2.67	2.00	1.00	0.68	0.42

The results summarized in Figures 3a, 4a and 5a show the comparison between authors' FE simulation and authors' analytical estimation of the temperature drop along the process. In Figures 3b, 4b and 5b, the comparison is made between authors' FE simulation and various literature models for the prediction of the radial forming force [4, 7, 8, 9] in which the inputted flow stress has been calculated utilizing (15).

In the material model defined by (15) the values of strain and strain rate have been derived using previous works of the authors [5, 6] whereas temperature has been calculated utilizing the models previously described in this paper.

The boundary conditions as well as the constants to use in the material model are resumed in Table 2. For all the cases the material is the steel alloy 42CrMo4, initially heated up to 1200 °C.

$$\sigma_F = C_1 \exp\left(C_2 \cdot T\right) \cdot \varepsilon^{\left(n_1 \cdot T + n_2\right)} \exp\left(\frac{L_1 \cdot T + L_2}{\varphi}\right) \dot{\varepsilon}^{\left(m_1 \cdot T + m_2\right)} \tag{15}$$

TABLE 2. Material 42CrMo4 model ranges and constants.

Parameter	Value	Parameter	Value
Temp. range [°C]	800 - 1250	n_2	0.20612
Strain range [-]	0.05 - 2	L_1	-8.26584e-5
Strain rate range [s^{-1}]	0.01 - 150	L_2	0.0289085
C_1	5290.47	m_1	0.000300752
C_2	-0.0036967	m_2	-0.156181
n_1	-0.000334025		

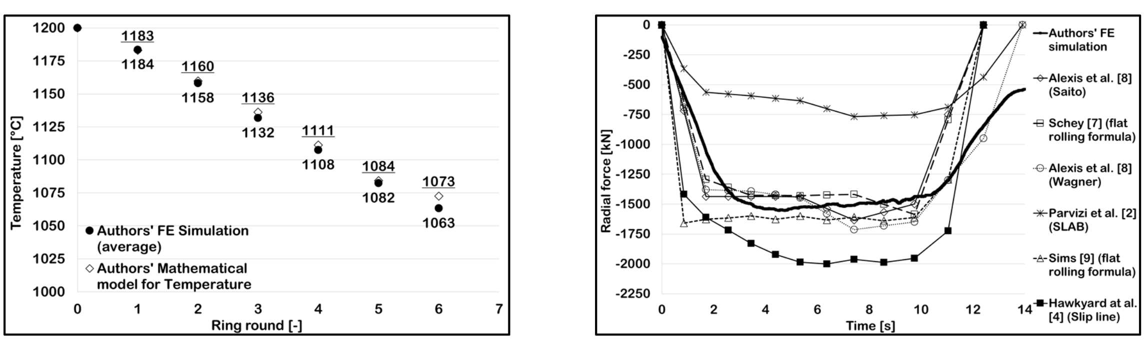

(a) (b)

FIGURE 3. (a) Temperature results comparison for RING1; (b) Force results comparison for RING1.

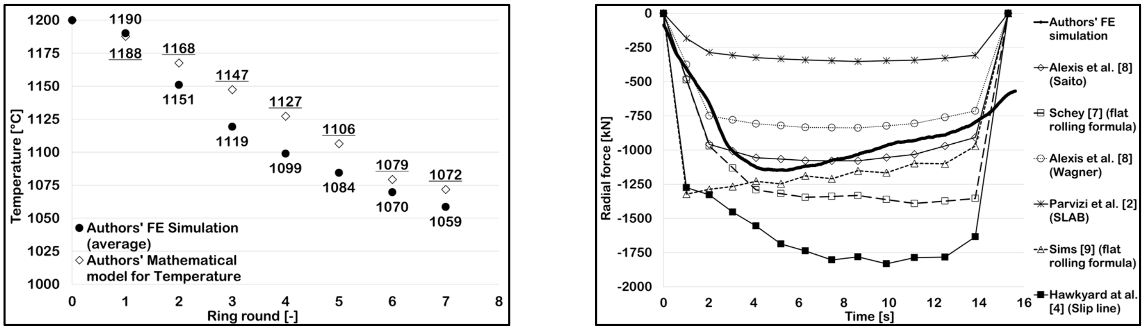

(a) (b)

FIGURE 4. (a) Temperature results comparison for RING3; (b) Force results comparison for RING3.

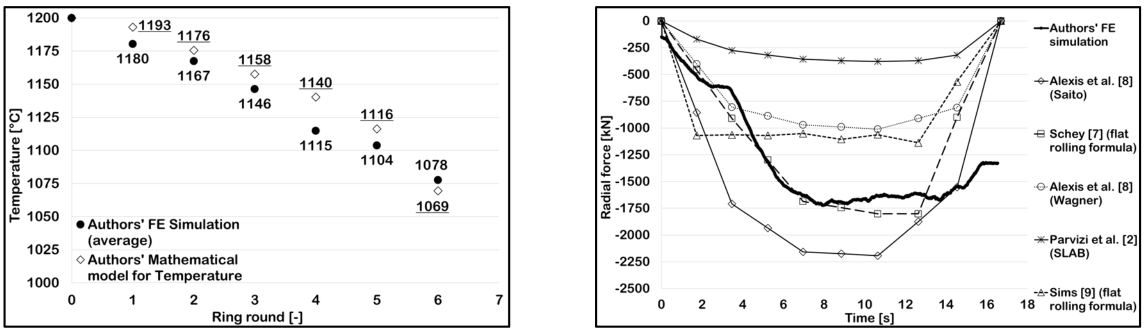

(a) (b)

FIGURE 5. (a) Temperature results comparison for RING5; (b) Force results comparison for RING5.

CONCLUSION

In all the analyzed cases, the maximum error of the temperature model at the end of the deformation process, respect to the average temperature between inner and outer surface estimated with FE simulation, is 1.23%, showing the reliability of the proposed model and its good integration with previous authors' works.

Regarding the prediction of the process forces, the application of literature models have shown that the lower the ratio between final height and thickness is, the higher the error and the spread of the models for the force prediction turns to be. This fact can be explained by some assumptions adopted for these models, which are normally a generalization of flat rolling or indenting process formulation adapted to ring rolling process.

If the ratio between ring height and thickness reaches values near 1 (RING3), or below (RING5), most of the analyzed literature models loose accuracy and, although the development of a model for the prediction of the process forces was out of the scope of this paper, this preliminary results encourages further analysis to develop an algorithm able to precisely foresee the process forces, superseding the highlighted limitations.

REFERENCES

1. G. Zhou, L. Hua and D.S. Qian, Comp. Mat. Sc. **50**, 911–924 (2011).
2. A. Parvizi, K. Abrinia and M. Salimi, J. of Mat. Eng. and Perf. **20**, 1505–1511 (2011).
3. A. Parvizi, K. Abrinia, Int. J. of Mech. Sc. **79**, 176–181 (2014).
4. J.B. Hawkyard, W. Johnson, J. Kirkland, E. Appleton, Int. J. of Mech. Sc. **15**, 873–893 (1973).
5. G.A. Berti, L. Quagliato, M. Monti, Int. J. of Mech. Sc. **99**, 58–71 (2015).
6. G.A. Berti and L. Quagliato, "Feasible setup definition and analytical strain estimation for radial-axial ring rolling process" in Proceedings of the 48th Plenary Meeting of the ICFG (2015), pp. 101–107.
7. J.A. Schey, in *Introduction to Manufacturing Processes*, edited by McGraw-Hill (3rd Edition, 2000), 319–370.
8. J.S. Alexis and X.A. Satheesh, Kovarenstvi (A Czech Republic International Journal) **24**, 11–17 (2004).
9. R.B. Sims, The calculation of Roll Force and Torque in Hot Rolling Mills, Proceeding of the Institution of Mechanical Engineers 1847–1982 (vol 1–196), 168, 191–200 (1954).